Improved noise performance of ultrathin YBCO Dayem bridge nanoSQUIDs

R Arpaia[1], M Arzeo[1], R Baghdadi[1], E Trabaldo[1], F Lombardi[1] and T Bauch[1]

[1] Quantum Device Physics Laboratory, Department of Microtechnology and Nanoscience, Chalmers University of Technology, S-41296 Göteborg, Sweden

E-mail: arpaia@chalmers.se and bauch@chalmers.se

Abstract. We have fabricated $YBa_2Cu_3O_{7-\delta}$ (YBCO) nano Superconducting QUantum Interference Devices (nanoSQUIDs), realized in Dayem bridge configuration, on films with thickness down to 10 nm. The devices, which have not been protected by a Au capping layer during the nanopatterning, show modulations of the critical current as a function of the externally applied magnetic field from 300 mK up to the critical temperature of the nanobridges. The absence of the Au shunting layer and the enhancement of the sheet resistance in ultrathin films lead to very large voltage modulations and transfer functions, which make these nanoSQUIDs highly sensitive devices. Indeed, by using bare YBCO nanostructures, we have revealed an upper limit for the intrinsic white flux noise level $S_{\Phi,w}^{1/2} < 450$ n$\Phi_0/\sqrt{\text{Hz}}$.

1. Introduction

During the last decade, research on nano Superconducting QUantum Interference Devices (nanoSQUIDs) has gained much interest, mainly with the aim of measuring the magnetic moments of very small spin systems and magnetic nanoparticles [1–20]. NanoSQUIDs made of High critical Temperature Superconductors (HTS) offer the additional advantage to be operated in strong magnetic fields [21–25].

On the boost of nanotechnologies applied to HTS to go beyond the present state of the art, we have recently shown the realization of the first $YBa_2Cu_3O_{7-\delta}$ (YBCO) nanoSQUIDs, realized in Dayem bridge configuration, working in the full temperature range up to the critical temperature T_C (≈ 83 K) [26]. On these devices, which are covered by a Au capping layer, used to minimize the damages introduced into the superconducting layer during the nanopatterning procedure, we have measured an ultra low white flux noise below 1 $\mu\Phi_0/\sqrt{\text{Hz}}$ above 10 kHz. Such value was limited by the electronics background noise, equal to $S_{\Phi,a}^{1/2} = S_{v,a}^{1/2}/V_\Phi$, where $S_{v,a}^{1/2}$ is the voltage noise density of our measurement setup (amplifiers and resistive lines) and V_Φ is the transfer function, derived from the slope of the voltage modulations as a function of the externally applied magnetic flux. Therefore, in order to lower this upper limit, and eventually

explore the intrinsic white flux noise level of our nanoSQUIDs, the value of the transfer function has to be increased.

To fulfill this goal, in this paper we report on the fabrication and characterization of YBCO Dayem bridge nanoSQUIDs, which are not covered by a Au layer. Such devices show higher differential resistances above the critical current I_C, with respect to their Au capped counterpart, both because the gold electric shunt is missing, and because we have also used ultrathin films, where the YBCO sheet resistance significantly increases when decreasing the thickness. This occurrence results in higher voltage modulations and larger transfer functions. Consequently, we have measured a white flux noise level of only $\simeq 450$ n$\Phi_0/\sqrt{\text{Hz}}$ above 100 kHz, which makes our devices very interesting for many aforementioned applications.

2. Film growth and nanopatterning procedure

Ultrathin *c*-axis oriented YBCO films, with thicknesses t from 50 nm down to 10 nm, are epitaxially grown by Pulsed Laser Deposition (PLD) on MgO (110) substrates. The films present smooth surfaces (the average roughness is at the order of one atomic cell); they are slightly overdoped, with an onset temperature of the superconducting transition $T_C^{onset} = 85$ K. The broadening ΔT of the superconducting transition is rather small for the 50 nm thick films ($\Delta T \approx 1$ K), while it increases by reducing the thickness. Such broadening, reducing the T_C^0 down to 77 K for the 10 nm thick films, has already been observed in previous works on ultrathin YBCO films [27–30]: an intrinsic size effect of the material, shrank at dimensions comparable with the superconducting coherence lenght ξ (~ 2 nm at zero temperature in the a-b plane), has been commonly taken into account, and the broadening has been consequently explained in terms of the Kosterlitz-Thouless (KT) transition related to vortex-antivortex pair dissociation in 2D systems [31, 32].

The nanostructures have been defined via pattern transfer through a hard mask and Ar^+ ion etching. However, with respect to the nanofabrication procedure described in our previous works [26, 33, 34], the Au capping layer has not been deposited on top of the YBCO films after the PLD deposition, for reasons which will be clarified in the following. The only protecting capping layer for the YBCO films during the patterning is the carbon hard mask, deposited by PLD at room temperature. The carbon layer protects YBCO from chemicals and from the direct impact of the Ar^+ ions during the etching. However it cannot prevent the heating of YBCO during the ion milling, because it is characterized by a thermal conductivity, which is much lower than that of YBCO. As a consequence of that, oxygen losses from the superconducting layer may occurr.

Our devices consist of two 100 nm long nanowires in parallel, whose width w is in the range 65 - 75 nm, connecting two 4 μm wide electrodes. The nanoSQUID loop is defined by the distance d_w between the wires, fixed to 1 μm, and by the distance between the electrodes d_e, equal to 250 nm. All the dimensions have been confirmed by scanning electron microscopy (see Fig. 1). The edges between the wires and the electrodes have been designed with a rounded shape in order to shorten the nanobridges, which brings

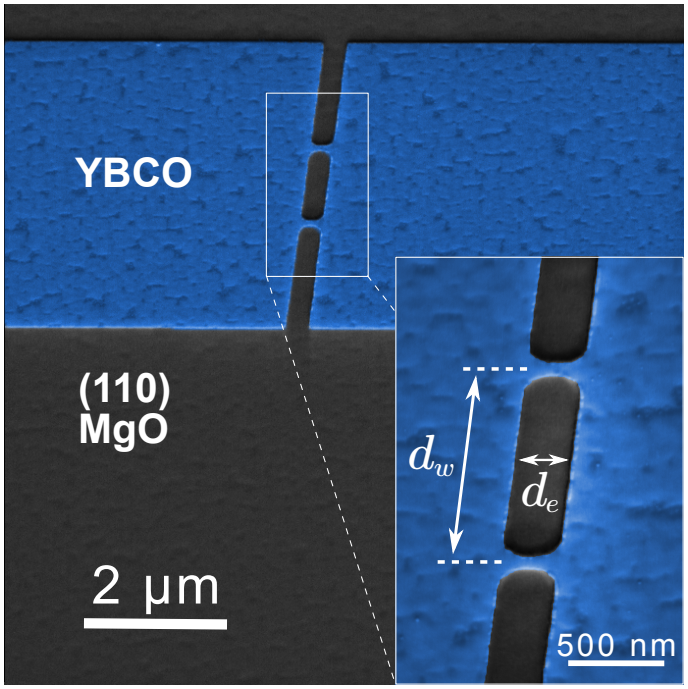

Figure 1. Scanning electron microscope image of the NSQ10, representative of our nanoSQUID geometry. Here, the superconducting loop (highlighted in the inset) is achieved on a bare 10 nm thick YBCO film by connecting two 4 μm wide electrodes with two 75 nm wide nanowires. The loop area, defined by the distance between the two electrodes d_e and by the distance between the nanowires d_w, is 250×1000 nm^2.

to a reduction of the kinetic inductance, without significantly reducing the loop area. The length l of the nanobridges is therefore smaller than the distance d_e between the electrodes.

In the following sections, the nanoSQUIDs of different thicknesses, realized on bare YBCO films, have been compared with a reference 50 nm thick YBCO nanoSQUID, NSQR, having the same geometry but covered by a 50 nm thick Au capping layer.

3. dc transport characterization

The electrical tranport properties of the nanoSQUIDs have been measured in a ^{3}He cryostat, shielded from ambient magnetic field. A 4-point measurement setup, with the current and voltage probes situated at the far ends of the two wide electrodes, has been used to record the current voltage characteristics (IVCs) of the devices from 300 mK up to their critical temperature, which is only few Kelvin lower than the T_C^0 of the unpatterned YBCO films. From the critical current I_C of the nanodevices, determined with a 2 μV criterium, we have extracted an average critical current density per wire, $J_C = I_C/(2wt)$, which is in the range $1 - 2.5 \cdot 10^7$ A/cm^2 independent of thickness, for all the investigated bare nanoSQUIDs (see Table 1). These values are about a factor two lower than those measured on devices having the same geometry but covered by a Au layer, preventing oxygen losses from the superconducting layer during the

nanopatterning procedure. The J_C reduction observed in bare YBCO nanoSQUIDs with respect to Au capped nanodevices is not very strong, implying the degradation of the superconducting properties due to the lack of Au is rather limited ‡. For comparison, we have measured in previous works a J_C reduction of one order of magnitude in bare YBCO nanowires where the Au capping was kept on top of the nanostructures during the nanopatterning, and then removed by a final Ar^+ ion etching [35, 36].

Similarly to what we have previously measured in Au capped YBCO nanoSQUIDs [26], our bare YBCO nanoSQUIDs exhibit modulations of the critical current I_C as a function of the externally applied magnetic field, from 300 mK (as in Fig. 2, related to the 10 nm thick nanoSQUID NSQ10) up to the critical temperature of the devices.

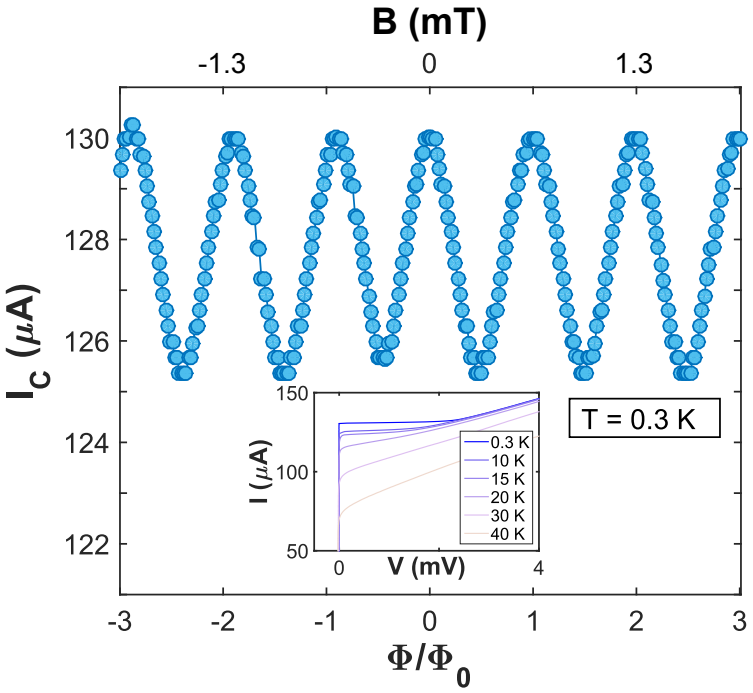

Figure 2. Critical current modulation of NSQ10 measured at $T = 300$ mK as a function of the applied magnetic field (*upper axis*) and magnetic flux (in unit of flux quantum, *lower axis*). In the inset, the IVC of the nanoSQUID is shown as a function of the temperature, from $T = 300$ mK up to $T = 40$ K. At the lowest temperatures the IVC is hysteretic, with a voltage switch of several mV above I_C driving the device to the normal state, characterized by a differential resistance $\delta R = 110\ \Omega$. The voltage switch decreases increasing the temperature, and the IVC is not anymore hysteretic at temperatures higher than 15 K.

From the application point of view, nonhysteretic IVCs are required, in order to use the nanoSQUIDs as magnetic flux to voltage transducers [37]. In addition, the voltage modulation at a fixed current bias point can be maximized, increasing the voltage responsivity to a magnetic flux variation, which in Dayem bridge SQUIDs can be

‡ Few devices, in particular the ultrathin ones, present properties which are negatively affected by the nanopatterning procedure, with J_C values as low as $6 \cdot 10^6$ A/cm^2. These devices have not been taken into consideration in the following for the noise investigation.

approximated by $\beta_L^{-1} \cdot I_C \cdot \delta R$, where β_L is the screening parameter, and δR the differential resistance measured above I_C [38]. Typically the β_L value for our nanoSQUIDs is around 20 at 4 K. We have already shown that the IVCs of our Au capped nanowires and nanoSQUIDs are flux flow like and nonhysteretic already at 300 mK, since the Au layer also acts as an electrical shunt [33]. As a consequence of that, the δR values are very small, since the resistance of the Au capped wires in the normal state is dominated by the resistance of the Au strips of length $l_{Au} = l$ on top of the two nanobridges.

Even though the Au capping layer is missing, the IVCs of all the investigated bare YBCO nanoSQUIDs with thicknesses larger than 10 nm are also nonhysteretic, mainly because of the high value of the thermal conductivity κ in YBCO [39] ($\kappa \approx 25$ $\mathrm{Wm^{-1}K^{-1}}$ in the normal state and at the optimally doped regime). This is a remarkable achievement, in particular for Dayem bridge nanoSQUIDs, showing often hysteretic IVCs [11,40,41]. The IVCs of the 10 nm thick nanoSQUIDs present instead a large voltage switch above I_C and are hysteretic, since at such small dimensions an hot spot regime is induced, driving all the system from the superconducting to the normal state. However, as shown in the inset of Figure 2, the voltage switch decreases when increasing the temperature, and the IVCs are nonhysteretic already at temperatures higher than 15 K. The δR values of all the investigated bare nanoSQUIDs are higher than those measured in the Au capped ones, therefore the product $\beta_L^{-1} \cdot I_C \cdot \delta R$, at a fixed thickness, improves. In particular, the choice of the 10 nm thick devices can be advantageous, since the increase of δR with respect to the thicker nanoSQUIDs is higher than the reduction of I_C: this is expected, since I_C scales as t, while the sheet resistance of YBCO, $R_\square$, which is similar to the differential resistance δR (see Table 1), does not scale as $1/t$, but it increases faster in ultrathin, almost 2D, films [29,32,42].

Device	**Au**	**t** (nm)	**w** (nm)	**l** (nm)	$\mathbf{I_C}$ (μA)	$\mathbf{J_C}$ (A/cm^2)	β_L	$\delta\mathbf{R}$ (Ω)	$R_\square$ (Ω)	$\mathbf{\Delta V_{max}}$ (mV)	$\mathbf{V_\Phi}$ (mV/Φ_0)	$\mathbf{S^{1/2}_{\Phi,w}}$ ($\mu\Phi_0/\sqrt{\mathrm{Hz}}$)
NSQ10	No	10	75	100	130	$1.0 \cdot 10^7$	23	110	130	0.65	3.6	<0.45
NSQ20	No	20	65	100	580	$2.2 \cdot 10^7$	24	19	33	0.45	2.7	-
NSQ50	No	50	65	100	1000	$1.5 \cdot 10^7$	20	13	12	0.42	2.2	<0.6
NSQR	Yes	50	65	100	2220	$3.4 \cdot 10^7$	18	1.5	4	0.2	1.5	<1

Table 1. Parameters of some investigated Dayem bridge nanoSQUIDs, characterized by different thicknesses t. The wires, whose lenght l and width w are obtained from SEM pictures, are not capped with Au layer, as those shown in our previous work [26]. NSQR is a device with Au capped nanowires, reported here for comparison. I_C, J_C, β_L and $\delta R = \partial V/\partial I$ are, respectively, the critical current of the device, the critical current density per wire, the screening parameter and the differential resistance, extracted from the IV characteristics at 4.2 K, with a voltage criterion of V=2 μV. $R_\square$ is the sheet resistance of the devices, measured at $T = 100$ K. ΔV_{max} is the maximum amplitude of the voltage modulations as a function of the externally applied magnetic field, at a given bias current; V_Φ is the value of the transfer function at the work point used for the noise measurement; $S_{\Phi,w}$ is the magnetic flux white noise upper limit of the device, as set by the electronics background noise. $\Delta V_{\max}$, V_Φ and $S_{\Phi,w}$ are measured at 4.2 K for devices NSQ20, NSQ50 and NSQR, while they are measured at 18 K for NSQ10, whose IVC is hysteretic up to 15 K (see inset of Fig. 2).

A summary of the most significative parameters measured on the bare YBCO nanoSQUIDs at different thicknesses, and their comparison with the results achieved on Au capped YBCO nanoSQUIDs, is reported in Table 1.

4. Noise measurements

Finally, we have measured the flux noise of our bare YBCO nanoSQUIDs. The noise spectra have been acquired operating the devices in open-loop mode, and using a cross correlation scheme [43]. The resulting amplifier input white noise level, including the Johnson-Nyquist noise of the resistive voltage lines connecting the devices at low temperature to the room temperature amplifiers, is $S_{v,a}^{1/2} \simeq 1.5$ nV/$\sqrt{\text{Hz}}$. To perform the measurements, each nanoSQUID has been biased at a current slightly above I_C and at a magnetic field maximizing the slope of the voltage modulations $V(\Phi)$. The maximum value of $\partial V/\partial\Phi$, V_Φ, called transfer function, is a crucial parameter, since the flux noise density $S_\Phi^{1/2}$ is evaluated from the measurement of the voltage noise density $S_V^{1/2}$ as $S_\Phi^{1/2} = S_V^{1/2}/V_\Phi$.

In our previous measurements on Au capped YBCO nanoSQUIDs, we have determined an upper limit $S_{\Phi,w}^{1/2} \simeq 0.7\,\mu\Phi_0/\sqrt{\text{Hz}}$ for the white noise of the devices above 10 KHz, which is determined by the electronics background noise $S_{\Phi,a}^{1/2} = S_{v,a}^{1/2}/V_\Phi$ [26]. Therefore, in order to lower this upper limit, and eventually explore the intrinsic white flux noise level of our nanoSQUIDs, the value of the transfer function has to be raised. This goal can be fulfilled by our bare YBCO nanoSQUIDs. In Figure 3 the voltage modulations at $T = 4.2$ K of one of our bare YBCO nanoSQUIDs (left panel) are shown at different bias currents, and compared to those observed at the same temperature on our reference SQUID (right panel), having the same geometry but capped by a Au layer. As a consequence of the larger δR, the voltage modulation is a factor two higher, leading to an enhanced transfer function V_Φ (see details in Table 1).

In Figure 4 (light blue diamonds) the magnetic flux noise spectral density, measured on the bare nanoSQUID NSQ10 at $T = 18$ K, where the IVC is nonhysteretic, is shown. The measurement is taken at a bias current $I_b = 117$ μA and at a flux bias (highlighted by the purple dot in the inset of Fig. 4) corresponding to a transfer function $V_\Phi = 3.6$ mV/Φ_0. This is the highest transfer function we have measured so far, as a consequence of the enhancement of the sheet resistance and of the differential resistance in sub-15 nm thick YBCO films. At frequencies above 100 kHz, the measured flux noise, which takes into account both the nanoSQUID flux noise and the electronics background noise, is $S_\Phi^{1/2} \simeq 0.6\,\mu\Phi_0/\sqrt{\text{Hz}}$. Therefore, from the measured value of the electronics background noise (see grey dots in Fig. 4) $S_{\Phi,a}^{1/2} \simeq 0.4\,\mu\Phi_0/\sqrt{\text{Hz}}$, we reach to an upper limit for the white noise of the device $S_{\Phi,w}^{1/2} = \sqrt{S_\Phi - S_{\Phi,a}} \simeq 450$ n$\Phi_0/\sqrt{\text{Hz}}$, which is almost a factor two lower than the best one reported in our previous work [26]. This flux noise value is less than one order of magnitude higher than the best values measured at 4.2 K in nanoSQUIDs made of Low critical Temperature Superconductors [14].

Below 100 kHz, the measured flux noise is strongly dependent on the frequency

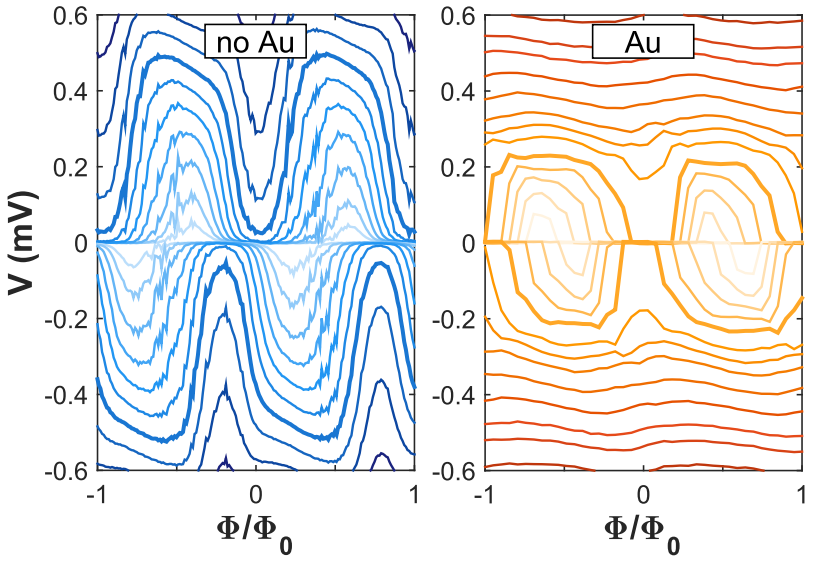

Figure 3. The voltage-flux modulations of the bare YBCO nanoSQUID NSQ20 (*left panel*) have been compared with those of the nanoSQUID NSQR (*right panel*), having similar geometry but covered by a Au capping layer. The different curves have been measured at dc bias currents $|I| = 584 - 612$ μA (in 3 μA steps) and $T = 4.2$ K for NSQ20, while at bias currents $|I| = 2250 - 2600$ μA (in 25 μA steps) and $T = 4.2$ K for NSQR. The maximum amplitude of the voltage modulations, $\Delta V_{\max}$, measured on the $V(\Phi)$ curve highlighed in bold, is roughly a factor 2 higher for the bare YBCO device. The transfer functions calculated on these two curves at the flux bias points corresponding to the maximum voltage responsivity yield $V_\Phi = 2.7$ mV/Φ_0 and $V_\Phi = 1.5$ mV/Φ_0 for the bare and for the capped device respectively (all the geometric and transport parameters related to these two nanoSQUIDs are listed in Table 1).

f. Such dependency can be nicely fitted (see blue line in Fig. 4) as $F^{1/2}(f) = \sqrt{\Sigma_{i=1}^{3} F_{L,i} + F_{1/f} + F_w}$ [44]. In the last expression, $\Sigma_{i=1}^{3} F_{L,i}^{1/2} = \Sigma_{i=1}^{3} F_{0,i}^{1/2}/[1 + (f/f_{c,i})^2]^{1/2}$ represents the sum of three Lorentzians having amplitudes $F_{0,1}^{1/2} = 110$ $\mu\Phi_0/\sqrt{\text{Hz}}$, $F_{0,2}^{1/2} = 17$ $\mu\Phi_0/\sqrt{\text{Hz}}$, $F_{0,1}^{1/2} = 8$ $\mu\Phi_0/\sqrt{\text{Hz}}$, and frequencies $f_{c,1} = 5$ Hz, $f_{c,2} = 2$ kHz, $f_{c,2} = 40$ kHz respectively, $F_{1/f}^{1/2}$ is a contribution proportional to $1/f^{1/2}$ and $F_w^{1/2} = 0.5$ $\mu\Phi_0/\sqrt{\text{Hz}}$ is a constant white noise term.

The noise spectrum shown in Figure 4 is independent of the choice of the flux bias. Therefore, we can attribute the measured $1/f$ dependency below 100 kHz on critical current fluctuations in our devices. Moreover the observed Lorentzians in the spectrum indicate the existence of strong localized two-level critical current fluctuators. To remove the contribution of critical current fluctuations, the SQUID has to be operated in flux-looked loop mode, using a bias reversal readout electronics [24, 45]. Both the removal of this low frequency componet to the measured noise, and the physical understanding of critical current fluctuations in YBCO nanowires - which is still unknown - go beyond the scope of this paper, and will be object of future works.

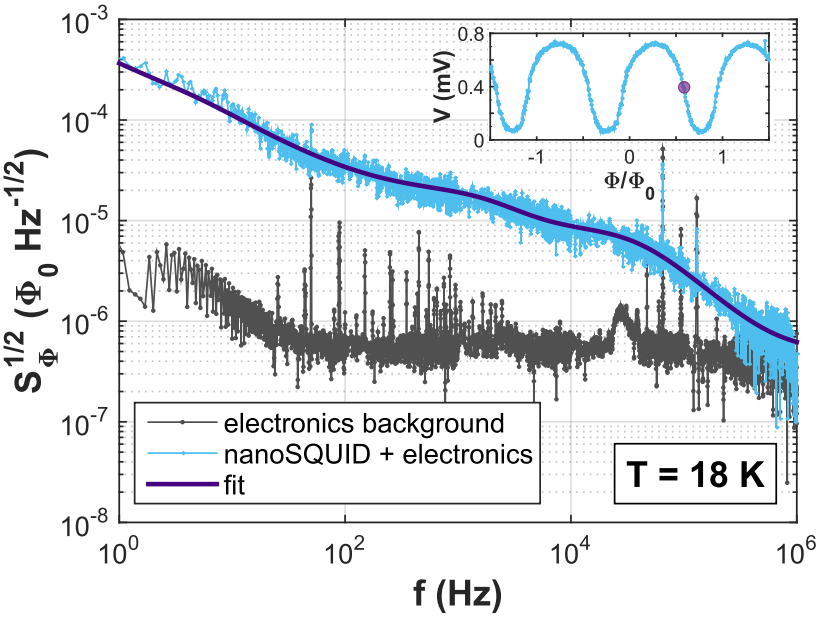

Figure 4. Magnetic flux noise spectral density $S_\Phi^{1/2}$ measured as a function of the frequency f on the nanoSQUID NSQ10 (light blue diamonds). The measurement is done at $T = 18$ K, where the IVC of the device is not hysteretic. The blue solid line is the fit to the $S_\Phi^{1/2}$ data with $F^{1/2}$, assuming the sum of three Lorentzians. Grey dots represent the electronics background noise. In the inset, the voltage-flux modulation measured at $T = 18$ K and $I_C = 120$ μA. The purple dot indicates the work point, corresponding to $V_\Phi = 3.6$ mV/Φ_0, where the noise spectrum has been taken.

5. Conclusions

In conclusion, we have fabricated YBCO Dayem bridge nanoSQUIDs, patterning films with thicknesses in the range $10 - 50$ nm. In the superconducting loop reside nanowires with cross section down to 75×10 nm. Differently from the previous devices we have realized in the same configuration [26, 46], the structures here are not covered by a Au capping layer. A carbon layer is instead deposited by PLD at room temperature directly on top of YBCO, acting both as a protecting layer and as a hard mask during the nanopatterning, and it then removed at the end of the fabrication. Despite the lack of the Au layer, the nanoSQUIDs show critical current modulations as a function of the external magnetic field in the whole temperature range below T_C^0, and critical current densities which are only slightly lower with respect to those of the best Au capped nanoSQUIDs previously measured. Furthermore, the bare YBCO nanoSQUIDs present voltage modulations - thence transfer functions - about a factor two larger than those of Au capped devices, as a consequence of their higher differential resistance δR measured above I_C. This results in a reduced upper limit of the white flux noise of our devices. In particular, on 10 nm thick nanoSQUIDs, where a further enhancement of the transfer function derives from the deviation of the sheet resistance from the linear $1/t$ dependence in ultrathin films, we have measured at 18 K a white flux noise level

of only $\simeq 450$ n$\Phi_0/\sqrt{\text{Hz}}$ above 100 kHz. The low noise level of our bare nanoSQUIDs makes them suitable for the detection of magnetic nanoparticles in moderate magnetic field and wide temperature range.

Acknowledgements

This work has been partially supported by the Swedish Research Council (VR) and the Knut and Alice Wallenberg Foundation.

References

[1] Lam S and Tilbrook D 2003 *Appl. Phys. Lett.* **82** 1078
[2] Gallop J 2003 *Supercond. Sci. Technol.* **16** 1575
[3] Hopkins D S, Pekker D, Goldbart P M and Bezryadin A 2005 *Science* **308** 1762–1765
[4] Cleuziou J P, Wernsdorfer W, Bouchiat V, Ondarçuhu T and Monthioux M 2006 *Nat. Nanotechnol.* **1** 53–59
[5] Troeman A G, Derking H, Borger B, Pleikies J, Veldhuis D and Hilgenkamp H 2007 *Nano Lett.* **7** 2152–2156
[6] Hao L, Macfarlane J, Gallop J, Cox D, Beyer J, Drung D and Schurig T 2008 *Appl. Phys. Lett.* **92** 192507
[7] Foley C and Hilgenkamp H 2009 *Supercond. Sci. Technol.* **22** 064001
[8] Bouchiat V 2009 *Supercond. Sci. Technol.* **22** 064002
[9] Wernsdorfer W 2009 *Supercond. Sci. Technol.* **22** 064013
[10] Giazotto F, Peltonen J T, Meschke M and Pekola J P 2010 *Nat. Phys.* **6** 254–259
[11] Vijay R, Levenson-Falk E, Slichter D and Siddiqi I 2010 *Appl. Phys. Lett.* **96** 223112
[12] Nagel J, Kieler O, Weimann T, Wölbing R, Kohlmann J, Zorin A, Kleiner R, Koelle D and Kemmler M 2011 *Appl. Phys. Lett.* **99** 032506
[13] Russo R, Granata C, Esposito E, Peddis D, Cannas C and Vettoliere A 2012 *Appl. Phys. Lett.* **101** 122601
[14] Vasyukov D, Anahory Y, Embon L, Halbertal D, Cuppens J, Neeman L, Finkler A, Segev Y, Myasoedov Y, Rappaport M L *et al.* 2013 *Nat. Nanotechnol.* **8** 639–644
[15] Granata C, Vettoliere A, Russo R, Fretto M, De Leo N and Lacquaniti V 2013 *Appl. Phys. Lett.* **103** 102602
[16] Hazra D, Kirtley J R and Hasselbach K 2014 *Appl. Phys. Lett.* **104** 152603
[17] Schmelz M, Matsui Y, Stolz R, Zakosarenko V, Schönau T, Anders S, Linzen S, Itozaki H and Meyer H 2015 *Supercond. Sci. Technol.* **28** 015004
[18] Granata C, Massarotti D, Vettoliere A, Fretto M, D'Ortenzi L, De Leo N, Stornaiulo D, Silvestrini P, Ruggiero B, Tafuri F *et al.* 2016 *IEEE Trans. Appl. Supercond.* **26** 1–5
[19] Sharon O J, Shaulov A, Berger J, Sharoni A and Yeshurun Y 2016 *Sci. Rep.* **6** 28320
[20] Granata C and Vettoliere A 2016 *Phys. Rep.* **614** 1–69
[21] Nagel J, Konovalenko K, Kemmler M, Turad M, Werner R, Kleisz E, Menzel S, Klingeler R, Büchner B, Kleiner R *et al.* 2010 *Supercond. Sci. Technol.* **24** 015015
[22] Schwarz T, Nagel J, Wolbing R, Kemmler M, Kleiner R and Koelle D 2012 *ACS Nano* **7** 844–850
[23] Wölbing R, Schwarz T, Müller B, Nagel J, Kemmler M, Kleiner R and Koelle D 2014 *Supercond. Sci. Technol.* **27** 125007
[24] Schwarz T, Wölbing R, Reiche C F, Müller B, Martínez-Pérez M J, Mühl T, Büchner B, Kleiner R and Koelle D 2015 *Phys. Rev. Applied* **3** 044011
[25] Charpentier S, Arpaia R, Gaudet J, Matte D, Baghdadi R, Löfwander T, Golubev D, Fournier P, Bauch T and Lombardi F 2016 *Phys. Rev. B* **94** 060503

[26] Arpaia R, Arzeo M, Nawaz S, Charpentier S, Lombardi F and Bauch T 2014 *Appl. Phys. Lett.* **104** 072603
[27] Chan I, Vier D, Nakamura O, Hasen J, Guimpel J, Schultz S and Schuller I K 1993 *Phys. Lett. A* **175** 241–245
[28] Savvides N and Katsaros A 1994 *Physica C* **226** 23–36
[29] Tang W, Ng C, Yau C and Gao J 2000 *Supercond. Sci. Technol.* **13** 580
[30] Probst P, Semenov A, Ries M, Hoehl A, Rieger P, Scheuring A, Judin V, Wünsch S, Il'in K, Smale N, Mathis Y L, Müller R, Ulm G, Wüstefeld G, Hübers H W, Hänisch J, Holzapfel B, Siegel M and Müller A S 2012 *Phys. Rev. B* **85** 174511
[31] Beasley M, Mooij J and Orlando T 1979 *Phys. Rev. Lett.* **42** 1165
[32] Matsuda Y, Komiyama S, Onogi T, Terashima T, Shimura K and Bando Y 1993 *Phys. Rev. B* **48** 10498
[33] Arpaia R, Nawaz S, Lombardi F and Bauch T 2013 *IEEE Trans. Appl. Supercond.* **23** 1101505–1101505
[34] Nawaz S, Arpaia R, Lombardi F and Bauch T 2013 *Phys. Rev. Lett.* **110** 167004
[35] Nawaz S, Arpaia R, Bauch T and Lombardi F 2013 *Physica C* **495** 33–38
[36] Arpaia R, Ejrnaes M, Parlato L, Cristiano R, Arzeo M, Bauch T, Nawaz S, Tafuri F, Pepe G and Lombardi F 2014 *Supercond. Sci. Technol.* **27** 044027
[37] Granata C, Vettoliere A, Russo R, Russo M and Ruggiero B 2011 *Phys. Rev. B* **83** 092504
[38] Rogalla H and Mück M 1987 *Jpn. J. Appl. Phys.* **26** 1645
[39] Sutherland M, Hawthorn D G, Hill R W, Ronning F, Wakimoto S, Zhang H, Proust C, Boaknin E, Lupien C, Taillefer L, Liang R, Bonn D A, Hardy W N, Gagnon R, Hussey N E, Kimura T, Nohara M and Takagi H 2003 *Phys. Rev. B* **67** 174520
[40] Wernsdorfer W, Mailly D and Benoit A 2000 *J. Appl. Phys.* **87** 5094–5096
[41] Hazra D, Kirtley J and Hasselbach K 2015 *Phys. Rev. Applied* **4** 024021
[42] Cieplak M Z, Guha S, Vadlamannati S, Giebultowicz T and Lindenfeld P 1994 *Phys. Rev. B* **50** 12876
[43] Sampietro M, Fasoli L and Ferrari G 1999 *Rev. Sci. Instrum.* **70** 2520–2525
[44] Arzeo M, Arpaia R, Baghdadi R, Lombardi F and Bauch T 2016 *J. Appl. Phys.* **119** 174501
[45] Drung D 2003 *Supercond. Sci. Technol.* **16** 1320
[46] Arpaia R, Golubev D, Baghdadi R, Arzeo M, Kunakova G, Charpentier S, Nawaz S, Lombardi F and Bauch T 2014 *Physica C* **506** 165–168